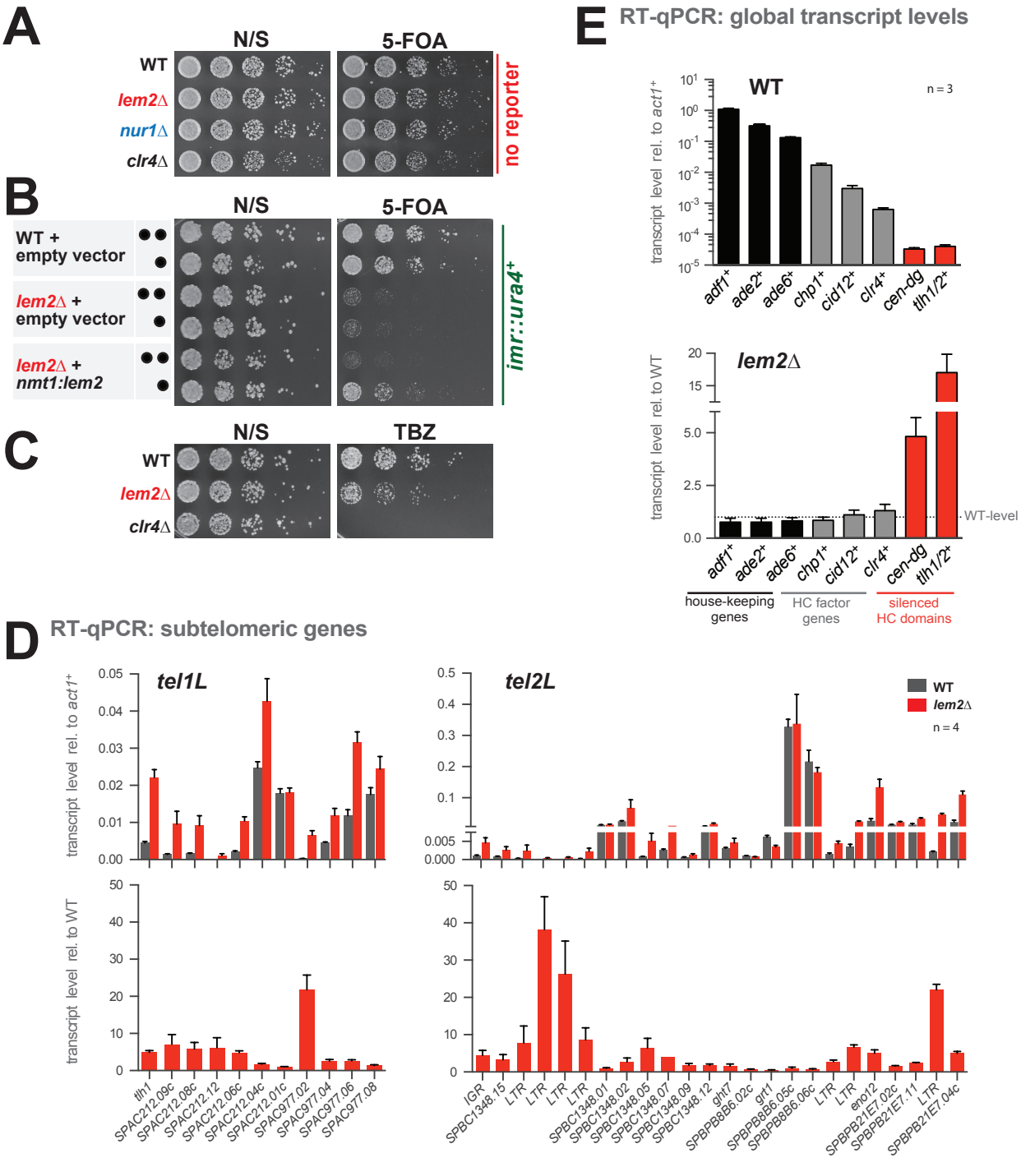
A
N/S
5-FOA
WT
lem2Δ
nur1Δ
clr4Δ
no reporter
B
N/S
5-FOA
WT + empty vector
lem2Δ + empty vector
lem2Δ + nmt1:lem2
imr::ura4+
C
N/S
TBZ
WT
lem2Δ
clr4Δ
E
RT-qPCR: global transcript levels
WT
n = 3
transcript level rel. to act1+
adf1+ ade2+ ade6+ chp1+ cid12+ clr4+ cen-dg tlh1/2+
lem2Δ
transcript level rel. to WT
WT-level
house-keeping genes
HC factor genes
silenced HC domains
D
RT-qPCR: subtelomeric genes
tel1L
tel2L
WT
lem2Δ
n = 4
transcript level rel. to act1+
transcript level rel. to WT
tlh1 SPAC212.09c SPAC212.08c SPAC212.12 SPAC212.06c SPAC212.04c SPAC212.01c SPAC977.02 SPAC977.04 SPAC977.06 SPAC977.08
IGR SPBC1348.15 LTR LTR LTR LTR SPBC1348.01 SPBC1348.02 SPBC1348.05 SPBC1348.07 SPBC1348.09 SPBC1348.12 ght7 SPBPB8B6.02c grt1 SPBPB8B6.05c SPBPB8B6.06c LTR LTR eno12 SPBPB21E7.02c SPBPB21E7.11 LTR SPBPB21E7.04c

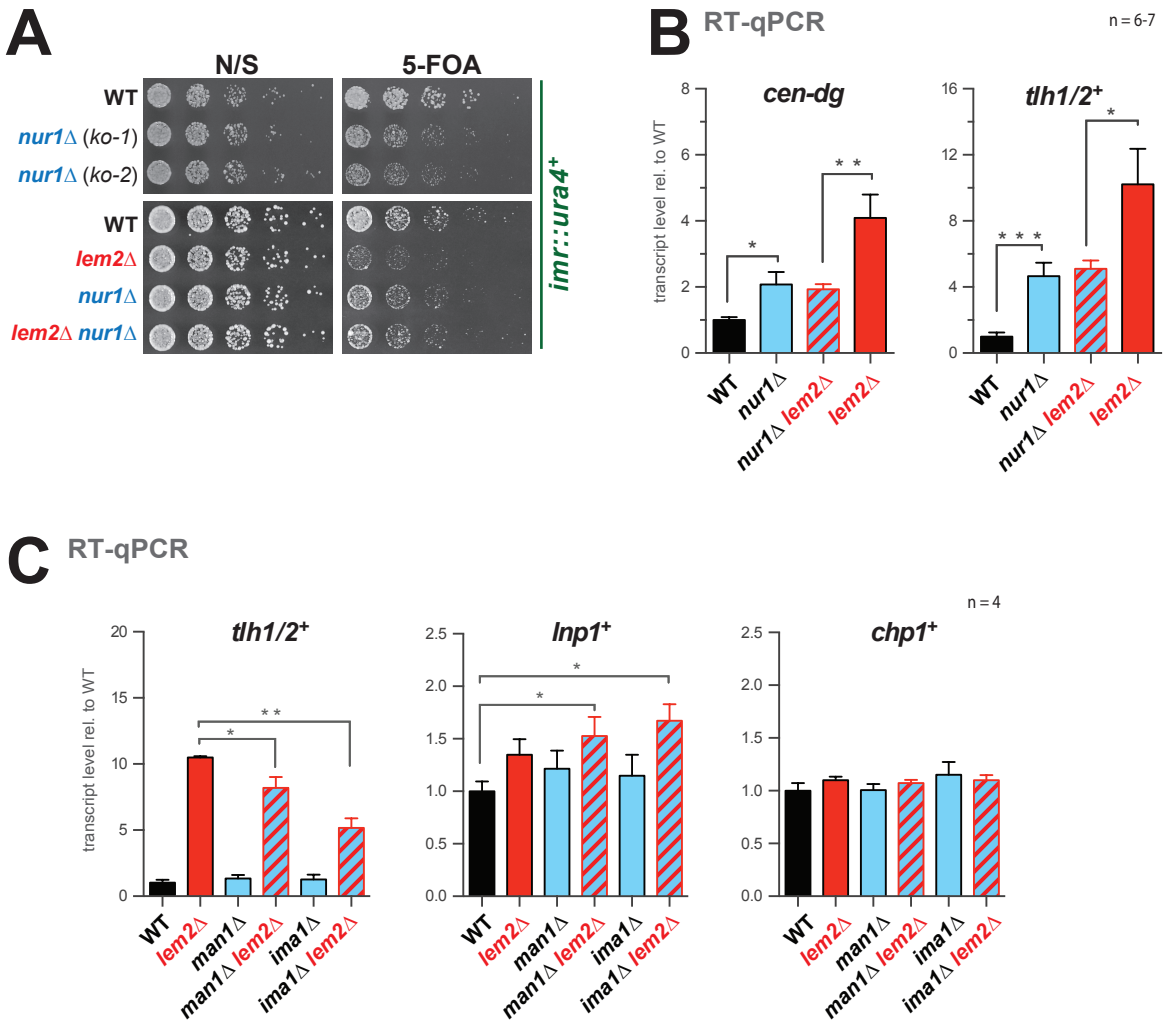
A
N/S
5-FOA
WT
nur1Δ (ko-1)
nur1Δ (ko-2)
WT
lem2Δ
nur1Δ
lem2Δ nur1Δ
imr::ura4+
B
RT-qPCR
n = 6-7
cen-dg
tlh1/2+
transcript level rel. to WT
WT
nur1Δ
nur1Δ lem2Δ
lem2Δ
C
RT-qPCR
n = 4
tlh1/2+
lnp1+
chp1+
transcript level rel. to WT
WT
lem2Δ
man1Δ
man1Δ lem2Δ
ima1Δ
ima1Δ lem2Δ

Barrales_SuppFig_S3

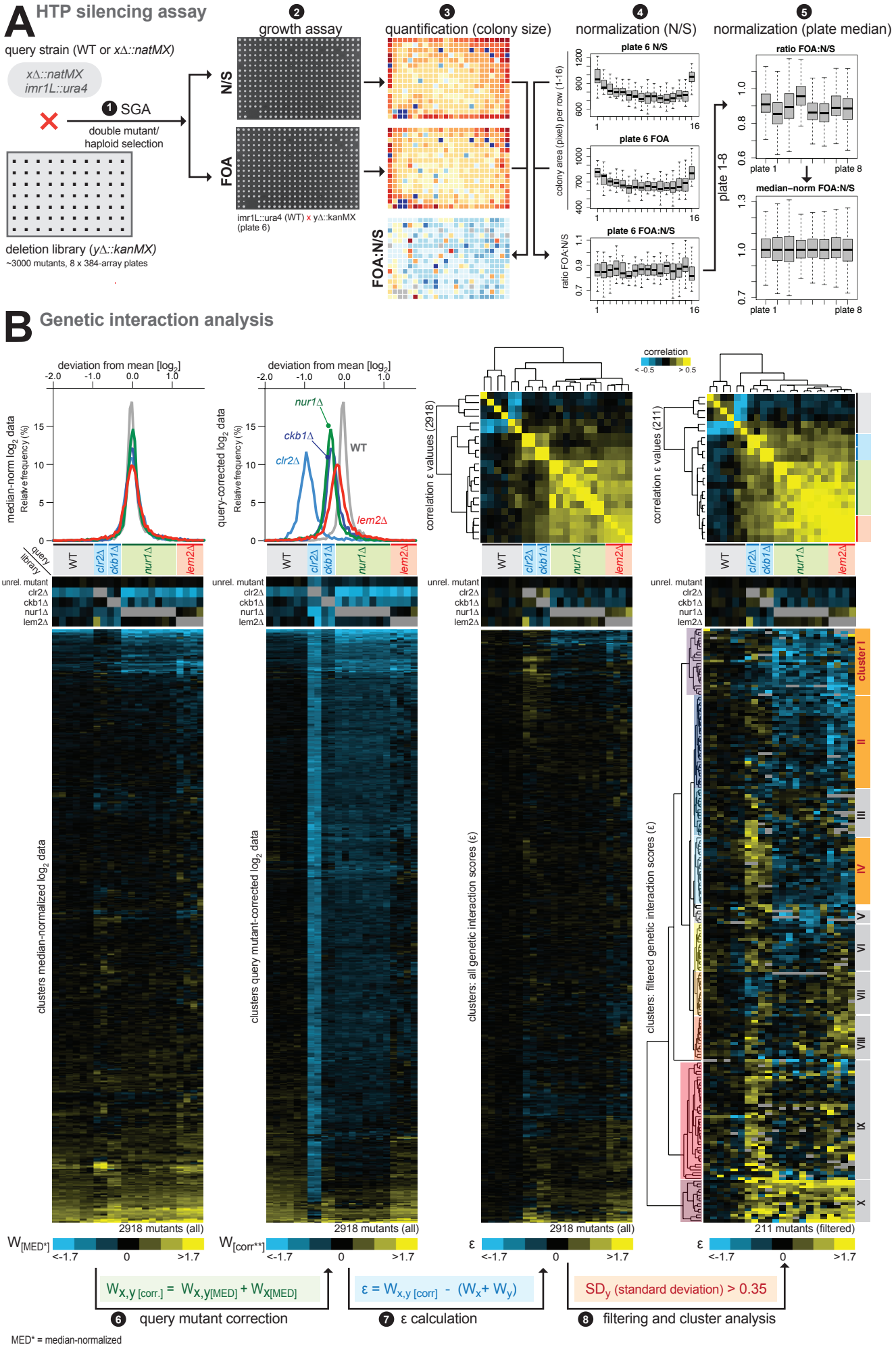

Barrales_SuppFig_S4

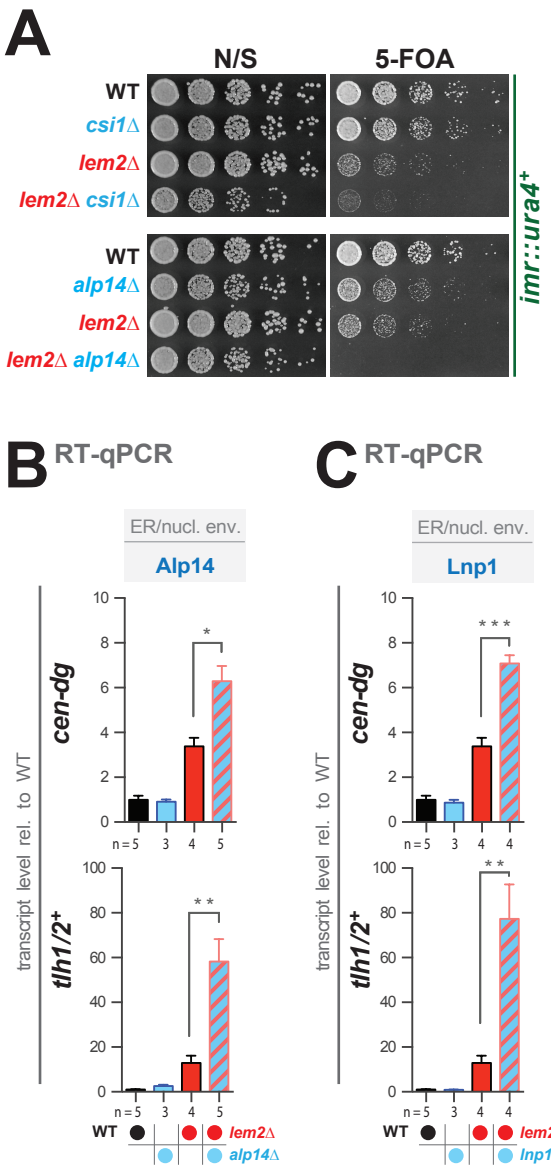

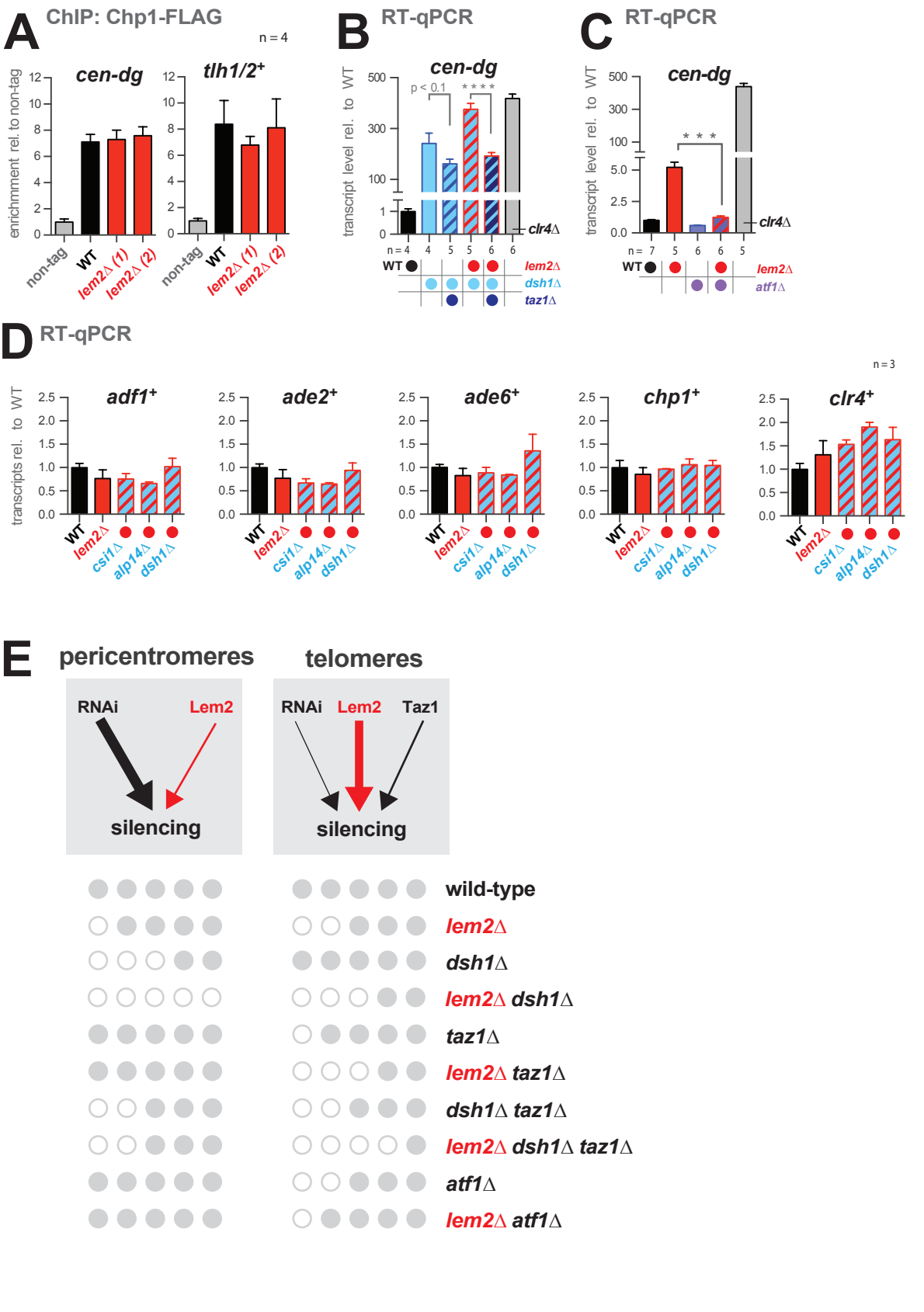
A
ChIP: Chp1-FLAG
n = 4
cen-dg
tlh1/2+
enrichmment rel. to non-tag
non-tag
WT
lem2Δ (1)
lem2Δ (2)
B
RT-qPCR
cen-dg
transcript level rel. to WT
p < 0.1
****
clr4Δ
lem2Δ
dsh1Δ
taz1Δ
C
RT-qPCR
cen-dg
transcript level rel. to WT
* * *
clr4Δ
lem2Δ
atf1Δ
D
RT-qPCR
n = 3
adf1+
ade2+
ade6+
chp1+
clr4+
transcripts rel. to WT
WT
lem2Δ
csi1Δ
alp14Δ
dsh1Δ
E
pericentromeres
telomeres
RNAi
Lem2
Taz1
silencing
wild-type
lem2Δ
dsh1Δ
lem2Δ dsh1Δ
taz1Δ
lem2Δ taz1Δ
dsh1Δ taz1Δ
lem2Δ dsh1Δ taz1Δ
atf1Δ
lem2Δ atf1Δ

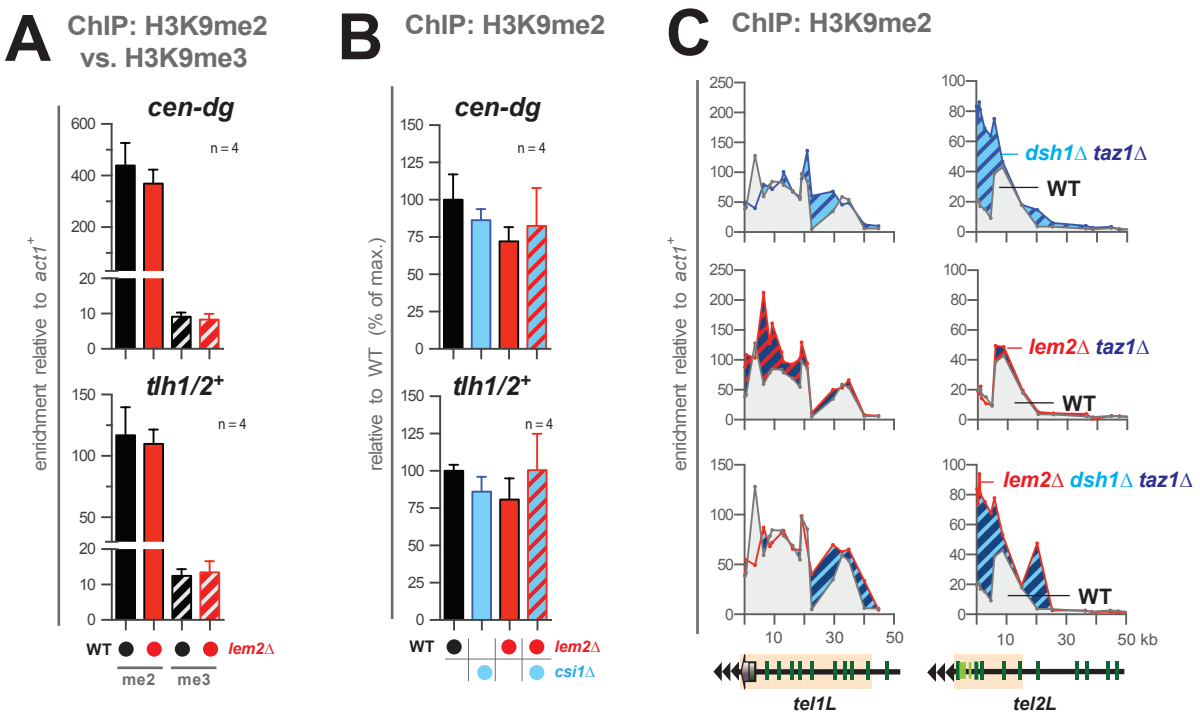
A
ChIP: H3K9me2 vs. H3K9me3
cen-dg
n = 4
tlh1/2+
n = 4
enrichment relative to act1+
WT
lem2Δ
me2
me3
B
ChIP: H3K9me2
cen-dg
n = 4
tlh1/2+
n = 4
relative to WT (% of max.)
WT
lem2Δ
csi1Δ
C
ChIP: H3K9me2
enrichment relative to act1+
dsh1Δ taz1Δ
WT
lem2Δ taz1Δ
WT
lem2Δ dsh1Δ taz1Δ
WT
10
30
50
50 kb
tel1L
tel2L

Barrales_SuppFig_S7

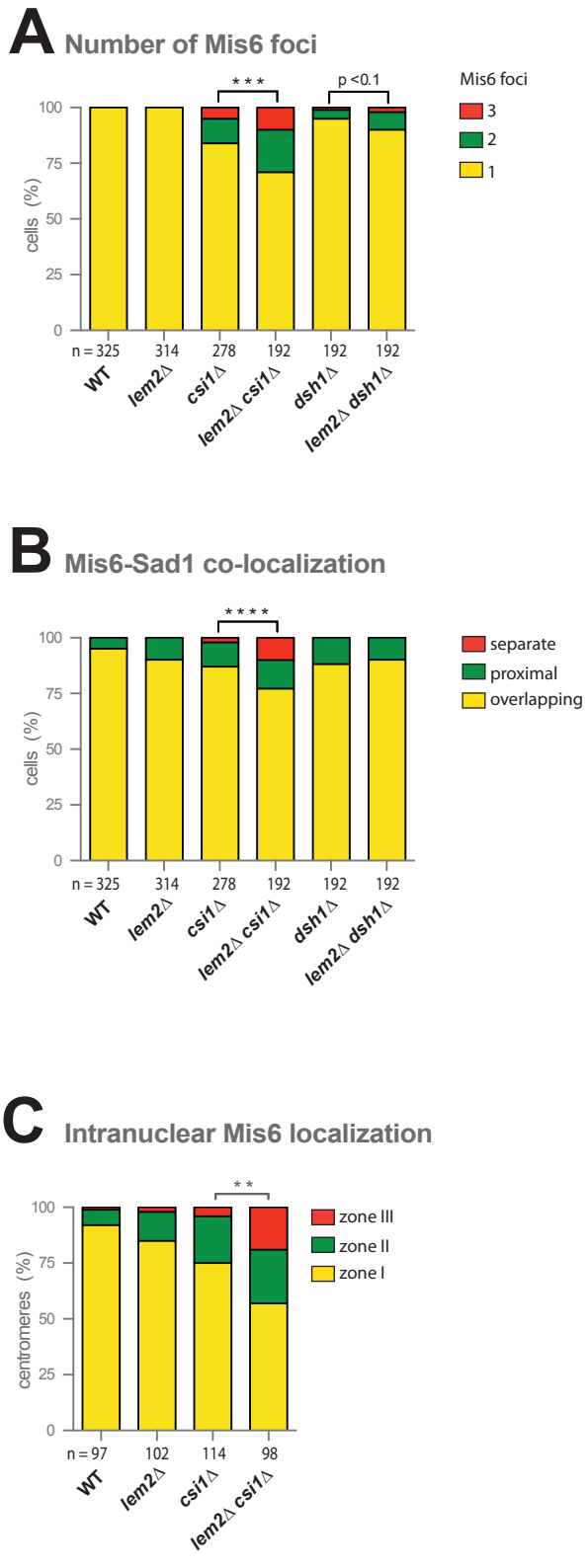

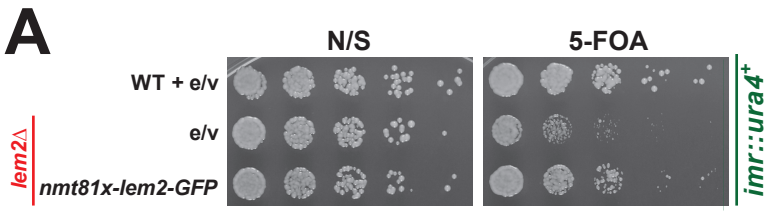
A
N/S
5-FOA
WT + e/v
e/v
nmt81x-lem2-GFP
lem2Δ
imr::ura4+

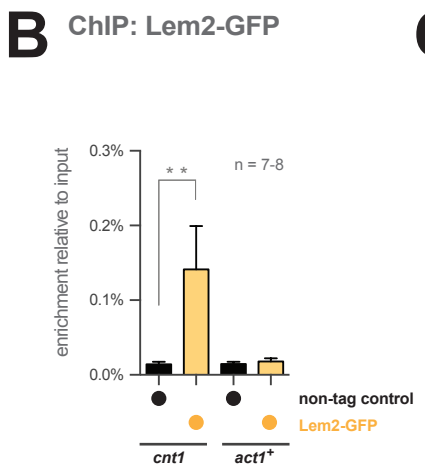
B
ChIP: Lem2-GFP
enrichment relative to input
0.3%
0.2%
0.1%
0.0%
n = 7-8
* *
non-tag control
Lem2-GFP
cnt1
act1+

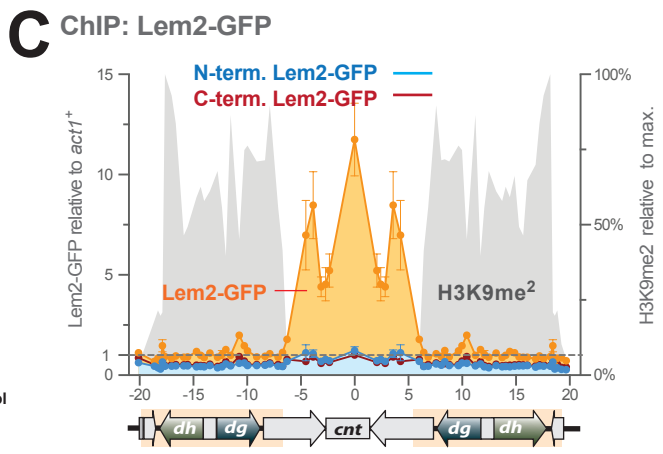
C
ChIP: Lem2-GFP
N-term. Lem2-GFP
C-term. Lem2-GFP
Lem2-GFP relative to act1+
H3K9me2 relative to max.
Lem2-GFP
H3K9me2
dh
dg
cnt
dg
dh

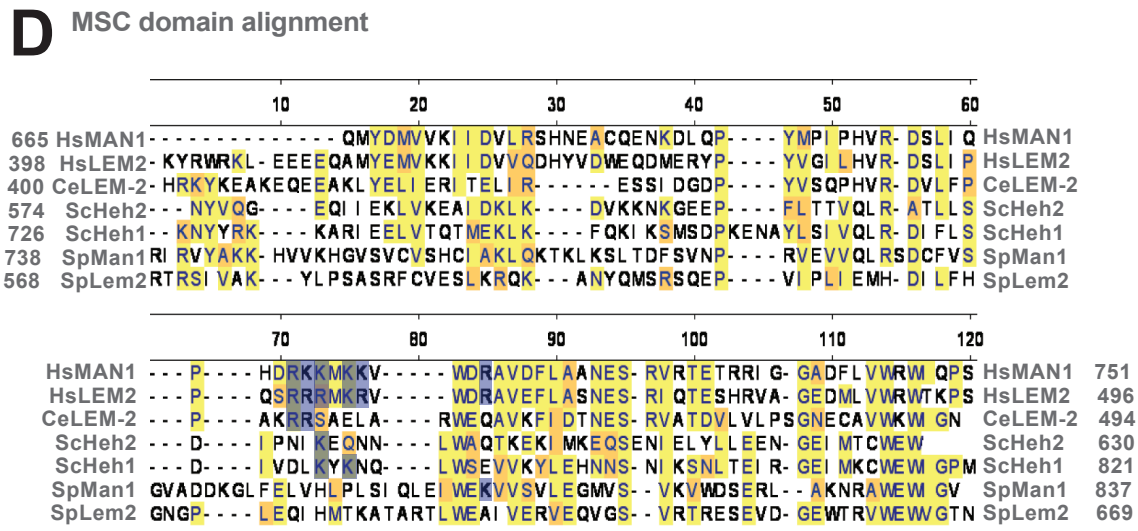
D
MSC domain alignment
HsMAN1
HsLEM2
CeLEM-2
ScHeh2
ScHeh1
SpMan1
SpLem2

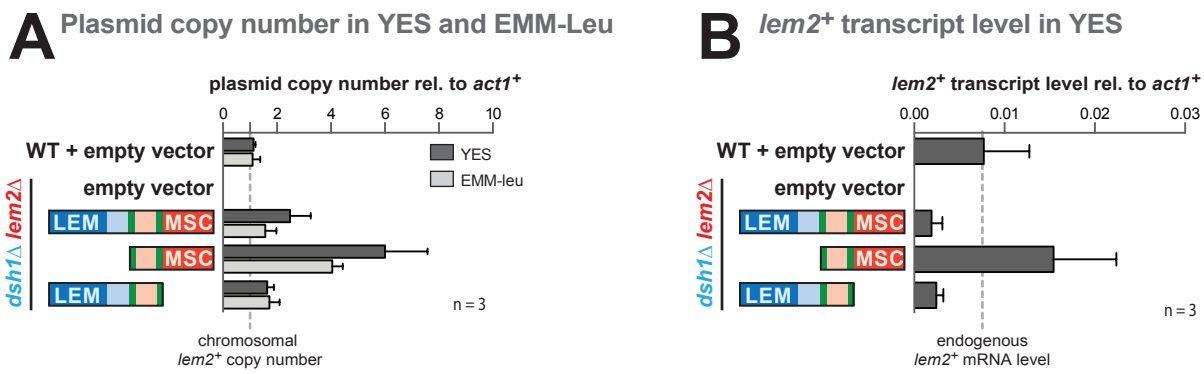
A
Plasmid copy number in YES and EMM-Leu
plasmid copy number rel. to act1+
0
2
4
6
8
10
WT + empty vector
empty vector
LEM
MSC
MSC
LEM
dsh1Δ lem2Δ
YES
EMM-leu
n = 3
chromosomal
lem2+ copy number
B
lem2+ transcript level rel. to act1+
0.00
0.01
0.02
0.03
WT + empty vector
empty vector
LEM
MSC
MSC
LEM
dsh1Δ lem2Δ
n = 3
endogenous
lem2+ mRNA level

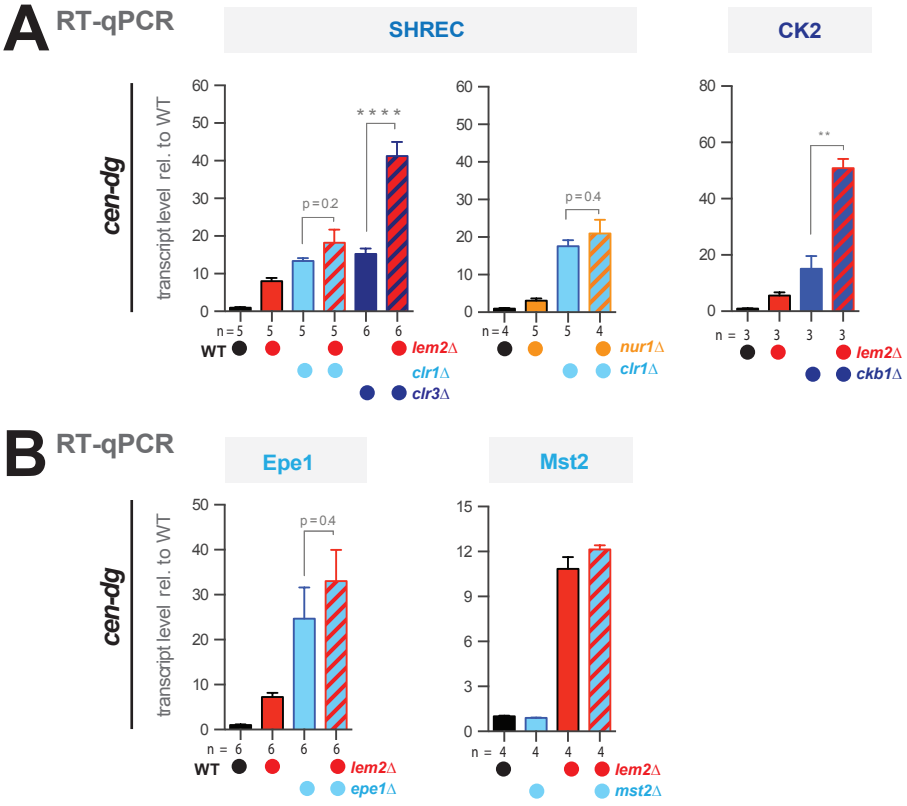
A
RT-qPCR
SHREC
CK2
cen-dg
transcript level rel. to WT
p=0.2
****
p=0.4
**
n=5 5 5 5 6 6
n=4 5 5 4
n= 3 3 3 3
WT
lem2Δ
clr1Δ
clr3Δ
nur1Δ
ckb1Δ
B
RT-qPCR
Epe1
Mst2
p=0.4
n= 6 6 6 6
n= 4 4 4 4
epe1Δ
mst2Δ

SUPPLEMENTAL FIGURE LEGENDS

Figure S1: Lem2 controls repression of silent chromatin but not generally transcription
(A) Growth assay on non-selective (N/S) and 5-FOA (5'-fluoroorotic acid) in absence of the *ura4*$^+$ reporter. Five-fold dilutions of WT cells and strains as indicated.
(B) Silencing reporter assay. Serial dilutions of WT and *lem2*Δ cells harboring empty vector or expressing full-length *lem2*$^+$ from the moderate *nmt41x* promoter (●●) or weak *nmt81x* promoter (●). Note that suppression is only seen when *lem2*$^+$ is expressed from the weak *nmt81x* promoter, suggesting that high cellular levels of Lem2 might be deleterious for silencing.
(C) Growth assay in the presence of 10 µg/ml thiabendazole (TBZ).
(D) RT-qPCR analysis of subtelomeric genes from the left (tel1L) and right (tel2R) arm of telomere 1 and 2, respectively. Top: Transcript levels relative to *act1*$^+$ in WT and *lem2*Δ cells. Bottom: Transcript levels relative to WT after normalization to *act1*$^+$ in *lem2*Δ cells.
(E) RT-qPCR analysis. Top: Transcript levels relative to *act1*$^+$ with error bars (SEM) in WT cells. Bottom: Transcript levels relative to WT after normalization to *act1*$^+$ in *lem2*Δ cells.
For all quantitative experiments: Data are represented as mean ± SEM from *n* independent experiments.

Figure S2: Lem2 acts together with Nur1 but independently of Man1 and Ima1
(A) Silencing reporter assay. Five-fold dilutions of WT cells and strains as indicated.
(B) and (C) RT-qPCR analysis of indicated transcripts. Shown are transcript levels relative to WT after normalization to *act1*$^+$.
For all quantitative experiments: Data are represented as mean ± SEM from *n* independent experiments; asterisks denote $p < 0.05$ (*), < 0.01 (**), and < 0.001 (***) from two-tailed Student's t-test analysis.

Figure S3: High-throughput analysis of genetic interactions based on silencing reporter assays
(A) High throughput (HTP) silencing assay pipeline. ❶ Cross of query mutant (*x*Δ*::natMX*, containing a *ura4*$^+$ marker inserted in the pericentromeric *imr* region) with the deletion library (*y*Δ*::kanMX*, 8 plates with ~ 384 mutants) and selection of haploid double mutants. ❷ Silencing assay based on colony growth on non-selective media (N/S) and 5'-fluoroorotic acid (FOA) containing plates. ❸ Quantification of growth on N/S and FOA media by determining colony sizes (area) of digitalized pictures. The heat map indicates colonies with large (red) and small colonies (blue) or empty spaces (dark blue) and reveals common plate effects before normalization (larger colonies at the edges of the plates due to increased availability of nutrients; shown is plate 6 as an example). ❹ Normalization of individual mutants and elimination of plate effects by determining the ratio of colony sizes between growth on FOA and N/S. Shown are box plot distributions for each of the 16 rows of a repre-

sentative 384 plate (plate 6). ❺ Plate normalization. Each plate was normalized to the median of all FOA:N/S values derived from this plate. Shown are box plot distributions for all 8 plates.
(B) Genetic interaction analysis. Left: Distribution of all plate median-normalized data for each query mutant (top) as well as heat maps of selected (middle) and all mutants (bottom) derived from crosses with WT strain and query mutants. Shown are $\log_2$ values from FOA:N/S-corrected growth data after plate median-normalization, $W_{[MED]}$. Negative and positive values are represented in blue and yellow, respectively; grey indicates missing or N/A data. ❻ To correct for the silencing phenotype of each query mutant (which is masked by the median-normalization), all median-normalized growth values of the double mutants, $W_{x,y[MED]}$, are corrected by the phenotype of the single query strain, $W_{x[MED]}$, resulting in the corrected FOA growth values, $W_{x,y[corr]}$ (second from left). ❼ To calculate the genetic interaction score ε, the deviation was determined between the corrected FOA growth values of the double mutant, $W_{x,y[corr]}$, and the sum of the FOA growth values of the corresponding single mutants, W_x and W_y (second from right). ❽ To select for robust genetic interactions, for each individual mutant (y) the standard deviation, SD_y, was calculated for the ε values of all query strains (x), and a cut-off > 0.35 was applied, resulting in the selection of 211 mutants. Right: The top panel shows the correlation matrix of the genetic interaction profiles. The middle panel shows genetic interaction scores for selected mutants. The bottom panel shows the hierarchical clustering of the genetic interaction data using Euclidean distance as the similarity metric and complete linkage as the clustering method (Gene Cluster 3.0).

Figure S4: Lem2 synergizes with nuclear membrane/ER and cytoskeletal factors in repressing silent chromatin
(A) Growth assay on non-selective media (EMM) and media containing 5'-fluoroorotic acid (EMM+5-FOA) with single and double mutants of indicated strains.
(B) and (C) RT-qPCR analysis of heterochromatic mRNAs of indicated strains. Transcript levels are normalized to *act1*$^+$ and presented relative to WT. Data are represented as mean ± SEM from *n* independent experiments; asterisks denote p < 0.05 (*), 0.01 (**), and 0.001 (***) from two-tailed Student's t-test analysis.

Figure S5: Lem2 is part of specific networks of redundant silencing pathways
(A) ChIP-qPCR analysis of Chp1-FLAG. Shown are enrichments relative to the non-tag control at the *cen-dg* and *tlh1/2*$^+$ loci.
(B) and (C) RT-qPCR analysis of pericentromeric transcripts of indicated strains.
(D) RT-qPCR analysis showing transcript levels of several euchromatic genes relative to WT (see also Fig. S1E).
For all experiments: Data are represented as mean ± SEM from *n* independent experiments; asterisks denote p < 0.001 (***) and 0.0001 (****) from two-tailed Student's t-test analysis.

(E) Scheme illustrating the main pathways controlling heterochromatin silencing at centromeres and telomeres. The strength of the contribution of each pathway is symbolized by the thickness of the arrow, whereas the strength of the silencing defects in various combinations of mutants is shown below by empty (de-repression) and filled circles (remaining silencing).

Figure S6: H3K9me2 and H3K9me3 levels in *lem2*Δ mutants

(A) ChIP-qPCR experiment showing pericentromeric and telomeric H3K9me2 and H3K9me3.

(B) ChIP-qPCR analysis of H3K9me2 levels at indicated heterochromatic regions. Values are shown relative to WT after *act1*$^+$ normalization.

For (A) and (B) data are represented as mean ± SEM from *n* independent experiments.

(C) ChIP-qPCR experiment showing subtelomeric H3K9me2 profiles. Values are shown as enrichment relative to a*ct1*$^+$. Shown is a representative experiment.

Figure S7: Lem2 cooperates predominantly with Csi1 in centromere localization

(A) Quantification of cells with distinct numbers of Mis6 foci. Shown is the percentage for a population of *n* cells. (***) indicates $p < 0.001$ (chi-square test). Lack of Dsh1 has a subtle effect on centromere clustering, which is slightly increased when Lem2 is additionally absent.

(B) Quantification of cells displaying distinct degrees of co-localization of Mis6-GFP and Sad1-mCherry. For each cell, the most proximal Mis6-GFP focus next to the SPB (Sad1-mCherry) is classified as overlapping, proximal or completely separated from the SPB. Shown is the percentage of *n* cells representing each type of localization. (****) indicates $p < 0.0001$ (chi-square test).

(C) Quantification of Mis6-GFP distribution relative to the nuclear periphery as done in Figure 4D and E. Shown is the percentage of centromeres for each nuclear zone for a population of *n* cells. (**) indicates $p < 0.01$ (chi-square test).

Figure S8: Lem2 binds to the central core domain of centromeres when localized at the nuclear periphery

(A) Silencing reporter assay. Serial dilutions of WT and *lem2*Δ cells harboring empty vector (e/v) or expressing full-length *lem2*$^+$ from the weak *nmt81x* promoter.

(B) ChIP efficiency of Lem2-GFP. Enrichment is shown in percentage relative to input material. *n* Indicates the number of biological replicates. The asterisks (**) denotes a $p < 0.01$ from Mann-Whitney test.

(C) ChIP-qPCR experiments showing the binding profiles of Lem2-GFP nucleoplasmic fragments. Left *y* axis represents binding relative to *act1*$^+$, right *y* axis represents H3K9me2 levels relative to the maximum of each domain in WT cells (H3K9me2 data taken from Figures 3C and 3D).

(D) Alignment of MSC domains of fission yeast Man1 and Lem2 and homologous domains from other species. Similarities are highlighted by orange and yellow shading. The stretch of six positively charged residues (highlighted in blue) is not conserved in the MSC domains of *S. pombe*.

Figure S9: Plasmid copy number and *lem2* transcript levels do not differ for full-length Lem2 and the truncated fragment lacking the C-terminal domain, Related to Figure 6

(A) Quantitative analysis of plasmid copy number in WT and *dsh1*Δ *lem2*Δ cells grown in minimal media without leucine (EMM-Leu) or in rich media (YES) for the last 4-5 generations. The relative plasmid copy number was determined by qPCR by probing the gene region of *lem2*$^+$ that encodes the lumenal domain present in all plasmid-borne fragments of Lem2. For WT cells harboring the empty plasmid, the chromosomal copy of *lem2*$^+$ was amplified. Values relative to *act1*$^+$ are presented.

(B) *lem2*$^+$ transcripts levels of cells grown in rich media (YES) were obtained by RT-qPCR. Shown are values relative to *act1*$^+$.

Error bars represent the standard error of mean of three biological replicates.

Figure S10: Relationship of Lem2 with SHREC and Epe1 regarding the repression of pericentromeric transcripts, Related to Figure 7

(A) and (B) RT-qPCR analysis of pericentromeric transcripts in indicated mutants. Shown are mean values normalized to *act1*$^+$ and relative to WT with error bars (SEM) from *n* independent experiments. The asterisks denote $p < 0.01$ (**) and 0.0001 (****) from two-tailed Student's t-test analyses.